JOURNAL OF PROTEOMICS 117 (2015) 70–85

Available online at www.sciencedirect.com

ScienceDirect

www.elsevier.com/locate/jprot

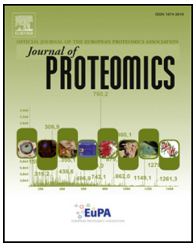

Dihydrolipoyl dehydrogenase as a potential UVB target in skin epidermis; using an integrated approach of label-free quantitative proteomics and targeted metabolite analysis

Eunjung Moon[a], *Hye Min Park*[b], *Choong Hwan Lee*[b], *Seon-Gil Do*[c], *Jong-Moon Park*[a], *Na-Young Han*[a], *Moon Ho Do*[a], *Jong Ha Lee*[a], *Hookeun Lee*[a,d,e,*], *Sun Yeou Kim*[a,d,**]

[a]*College of Pharmacy, Gachon University, Incheon, Republic of Korea*
[b]*Department of Bioscience and Biotechnology, Konkuk University, Seoul, Republic of Korea*
[c]*Life Science Research Institute, Univera, Inc., Seoul, Republic of Korea*
[d]*Gachon Medical Research Institute, Gil Medical Center, Incheon, Republic of Korea*
[e]*Lee Gil Ya Cancer and Diabetes Institute, Gachon University, Incheon, Republic of Korea*

ARTICLE INFO

Article history:
Received 10 May 2014
Accepted 12 December 2014

Keywords:
Integration of proteomics and targeted metabolite analysis
UVB targets
Photoaging
Epidermis
Dihydrolipoyl dehydrogenase
Aloe vera

ABSTRACT

Photodamage is extrinsically induced by overexposure to ultraviolet (UV) radiation, and it increases the risk of various skin disorders. Therefore, discovery of novel biomarkers of photodamage is important. In this study, using LC–MS/MS analysis of epidermis from UVB-irradiated hairless mice, we identified 57 proteins whose levels changed after UVB exposure, and selected 7 proteins related to the tricarboxylic acid (TCA) cycle through pathway analysis. Dihydrolipoyl dehydrogenase (DLD) was the only TCA cycle-associated protein that showed a decreased expression after the UVB exposure. We also performed targeted analysis to detect intermediates and products of the TCA cycle using GC–TOF-MS. Interestingly, malic acid and fumaric acid levels significantly decreased in the UVB-treated group. Our results demonstrate that DLD and its associated metabolites, malic acid and fumaric acid, may be candidate biomarkers of UVB-induced skin photoaging. Additionally, we showed that *Aloe vera*, a natural skin moisturizer, regulated DLD, malic acid and fumaric acid levels in UVB-exposed epidermis. Our strategy to integrate the proteome and targeted metabolite to detect novel UVB targets will lead to a better understanding of skin

Abbreviations: DLD, dihydrolipoyl dehydrogenase; DMEM, Dulbecco's modified Eagle's medium; FASP, filter-aided sample preparation; FBS, fetal bovine serum; HBSS, Hank's balanced salt solution; IPA, ingenuity pathway analysis; IVN, involucrin; MMP-1, matrix metalloproteinase-1; PC-1, procollagen type 1; PS, penicillin–streptomycin; ROS, reactive oxygen species; SA-β-Gal, senescence-associated β-galactosidase; SDS, sodium dodecyl sulfate; SNR, signal-to-noise ratio; TBST, Tris-buffered saline-T; TCA cycle, tricarboxylic acid cycle; UV, ultraviolet.

* *Correspondence to:* H. Lee, Gachon Medical Research Institute, Gil Medical Center, Incheon, Republic of Korea. Tel.: +82 32 899 6584; fax:+82 32 899 6519.
** *Correspondence to:* S.Y. Kim, College of Pharmacy, Gachon University, Incheon, Republic of Korea. Tel.: +82 32 899 6411; fax: +82 32 899 6591.
E-mail addresses: jubbi@hanmail.net (E. Moon), ramgee@naver.com (H.M. Park), chlee123@konkuk.ac.kr (C.H. Lee), sgildo@univera.com (S.-G. Do), bio4647@naver.com (J.-M. Park), ddasehan@nate.com (N.-Y. Han), dvmoono@naver.com (M.H. Do), whdgkfl@naver.com (J.H. Lee), hklee@gachon.ac.kr (H. Lee), sunnykim@gachon.ac.kr (S.Y. Kim).

http://dx.doi.org/10.1016/j.jprot.2014.12.016
1874-3919/

photoaging and photodamage. Our study also supports that *A. vera* exerts significant anti-photodamage activity via regulation of DLD, a novel UVB target, in the epidermis.

Biological significance
This study is the first example of an integration of proteomic and metabolite analysis techniques to find new biomarker candidates for the regulation of the UVB-induced skin photoaging. DLD, malic acid, and fumaric acid can be used for development of cosmeceuticals and nutraceuticals regulating the change of skin metabolism induced by the UVB overexposure. Moreover, this is also the first attempt to investigate the role of the TCA cycle in photodamaged epidermis. Our integration of the proteomic and targeted metabolite analyses will lead to a better understanding of the unidentified photobiological results from UVB-irradiated models and can elicit new diagnostic and treatment strategies based on altered metabolism.

1. Introduction

Overexposure to stimuli, such as solar radiation, smoking, and air pollutants are linked to skin damage. In particular, chronic and repeated exposure to ultraviolet (UV) radiation is the primary pathological factor in extrinsic skin photodamage and its complications [1,2]. Photodamage induces photoaging, which is a serious cosmetic problem for people concerned about beauty and skin care, and is characterized by a leathery appearance with wrinkles, loss of elasticity and collagen, depigmentation, and dryness [3]. Moreover, in recent years, due to the destruction of the ozone layer, the risk of skin photodamage complications such as skin cancer, melasma and inflammation, is increased by excessive UV exposure to the skin. Although many researchers have focused on skin problems caused by UV irradiation, there have been difficulties in developing a complete and unified picture of skin pathology. Until now, little attempts have been made to use reliable and robust technical approaches.

In this study, we have applied proteomics approach to reveal comprehensive features of skin photodamage and photoaging at the molecular level and to discover potential diagnostic biomarkers. In skin research, the 'omics' approach was initiated a decade ago [4] when Huang et al. first attempted skin proteomic analysis by characterizing the murine skin proteome [5]. They constructed a functional skin proteome database describing the protein networks that underlie biological processes. Edward et al. showed that different profiles of proteins were expressed in the skin of high-fat fed diabetic mice, compared to those of non-diabetic control mice [6]. Millioni et al. reported on the protein expression differences between cytoskeletal related proteins in cultured skin fibroblasts from type 1 diabetic patients with and without nephropathy [7]. Several studies have reported proteomic analysis of skin photodamage caused by UV irradiation of skin cells and tissues. The actin cytoskeleton modulators, cofilin-1 and destrin, were phosphorylated in human epidermis after UV irradiation [8]. In skin fibroblasts, the expressions of the nucleolar proteins, nucleophosmin and lysosomal cysteine–protease cathepsin B, were altered by UVA irradiation [9], and receptor-interacting protein and vimentin were altered by UVB [10].

Metabolomics-based skin research is still in the beginning stages. Fedele et al. reported on the prognostic relationship of B16F10's metabolic profile, possibly providing melanoma biomarkers [11]. Hu et al. showed the metabolomic response of human skin tissue to low dose ionizing radiation (IR) [12]. These studies can help with the understanding of the physiological changes after photodamage and identify biomarkers. Recently, Abaffty's group reported that comparative analysis of volatile organic compound metabolomics might be a potential tool to find biomarkers of skin cancer [13].

Kimball suggested that genomics, proteomics, and metabolomics were yielding challenging and important insights into unidentified skin biology and skin disease [14]. Until now, skin research based on metabolomics has been focused mainly on skin cancer. There is little report on biomarker discovery-based applications of multiple analyses for UVR skin photoaging and photodamage. Therefore, in order to find new biomarkers that can be applied in clinical practice, new methodology, such as an integration of proteomic and targeted metabolite analysis techniques, is needed. In this study, we have employed a liquid chromatography–mass spectrometry (LC–MS) based proteomic method and a gas chromatography MS (GC–MS) based targeted metabolite analysis to obtain insightful information regarding the expressed protein pattern of normal and UVB-irradiated epidermis from hairless mice, and to examine the TCA cycle-associated metabolites. Up to now, targeted metabolite analysis supports the proteomics data from photoaged skin tissue. However, this study using proteomics and a targeted metabolite analysis approach is the first attempt in the field to discover novel biomarker candidates for the diagnosis of photoaging and photodamage in UVB-exposed epidermis. In addition, we attempt to applicate the novel UVB-targets in *Aloe vera*-treated photoaged skin.

2. Materials and methods

2.1. Reagents

Hank's balanced salt solution (HBSS), fetal bovine serum (FBS), Dulbecco's modified Eagle's medium (DMEM), and penicillin–streptomycin (PS) were purchased from Gibco-BRL (Gaithersburg, MD, USA). Dispase was obtained from Roche (Basel, Switzerland). *Aloe vera* (*A. vera*) extract was provided by Univera Inc. (Seoul, Korea). Retinyl palmitate was purchased from Sigma Chemical

Co. (St. Louis, MO, USA). Primary and secondary antibodies were purchased from Santa Cruz Biotechnology (Delaware Ave, CA, USA).

2.2. Animal experiment

We purchased six-week-old Hos:HR-1 hairless mice (20–24 g) from Japan Shizuoka Laboratory Center Inc. (Hamamatsu, Japan). The male mice were chosen to mitigate the effect of the intrinsic factors such as a menstrual cycle and sex hormones in our study. Moreover, according to a previous study published in 2011 by Oh et al. [15], the epidermis of female skin was more sensitive than male skin due to intrinsic aging (the decrease in hyaluronic acid, sulfated glycosaminoglycans, urocanic acid, and water content), while the changes in the epidermal skin contents (decrease in sulfated glycosaminoglycans and water contents) by photoaging were observed in males. Namely, the sex in which significant changes can be observed in the epidermal skin by photoaging seems to be male. Overall, we considered that male hairless mice may be a more suitable animal model for achieving the aim of our study—the discovery of novel specific biomarkers of photoaging—than female mice. Mice were kept using a modification of the animal care protocol reported by Cozzi et al. [16]. To protect from the various stress responses induced by any fighting and injury, two mice were kept per cage, and separated by a physical barrier (opaque plastic panel). Animals were kept in a 23 °C and 65% humidity-controlled animal room with 12 h light/dark cycles. All procedures for animal experiments were reviewed and approved by the Animal Care Committee of the Center of Animal Care and Use at the Lee Gil Ya Cancer and Diabetes Institute, Gachon University, Korea (No. LCDI-2013-0022). The mice were allowed to adapt to their surroundings for at least seven days before beginning the experiments. During the experimental period, the mice were allowed free access to food and water. UVR includes UVA (320–400 nm), UVB (290–320 nm), and UVC (100–290 nm). Since UVC is blocked by dioxygen or ozone in the atmosphere and long wave UVA is less energetic than medium wave UVB, UVB has been thought to be responsible for the damaging effects in the skin. Therefore, we used a UVB lamp apparatus (BLX-312, Vilber Lourmal, France) for construction of a photoaged skin animal model in this study. We randomly divided 40 hairless mice into 4 groups of 10 mice: no UVB exposure (normal), UVB irradiation (UVB), UVB + aloe extract-treated (AE), and UVB + retinyl palmitate-treated (RP) groups. We constructed our skin photoaged animal model on the basis of the experimental methods of our published studies [17–19]. The mice were exposed to UVB radiation once per day at 200 mJ/cm^2 for the first week. Then, 400 mJ/cm^2 of UVB and topical application of samples were applied three times a week for 3 weeks. *A. vera* extracts (5%), retinyl palmitate (1%), and vehicle were applied on the dorsal skin of hairless mice. In this study, we used a solvent mixture of 70% propylene glycol and 30% ethanol as a vehicle. This solvent mixture is commonly used for the development of new topical formulations [20–22]. We topically applied all samples (500 μL/each mouse) on the dorsal skin of mice, and then gave enough time to be absorbed into the skin (about 30 min). The skin care product retinyl palmitate was used as the positive control (FDA, 2000). At the end of the study, we euthanized the mice in a humane way, minimizing their pain, by placing them in a CO_2 chamber for 5 min. Then, skin specimens from the central dorsum of the mice were obtained.

2.3. Histological and immunohistochemical analysis of the skin

The mice were sacrificed after the final UVB exposure and biopsies were obtained from the dorsal skin. The biopsies were fixed in 10% neutral buffered formalin for 24 h, embedded in paraffin and sectioned in 4 μm slices. The sections were stained with hematoxylin and eosin. Other samples were stained with Masson's trichrome to examine collagen density in the dermis. The stained slides were examined with a light microscope. For immunohistochemical analysis, tissue sections were incubated with specific antibodies against dihydrolipoyl dehydrogenase (DLD) for 16 h at 4 °C. Then, the tissues were stained with an Alexa-Fluor® 488 conjugated rabbit polyclonal antibody. Sections were mounted with VECTASHIELD® mounting media, and visualized using fluorescence microscopy.

2.4. Mouse skin tissue preparation for proteomic analysis

Segments of skin (approximately 2 × 2 cm^2) were excised from each mouse. Skin tissues were incubated in 1.5 mg/mL dispase in HBSS at 4 °C overnight, and separated into the epidermis and the dermis using forceps. The epidermal tissues were collected and homogenized using the CryoPrep™ system (Covaris, USA). Proteins were extracted using the Covaris S-series (Covaris, USA) in lysis buffer containing 8 M Urea, and 0.1 M Tri–HCl at pH 8.5. We used the epidermal skin tissue lysates pooled from three hairless mice [23]. Protein concentration was determined by the BCA Protein Assay Kit (Thermo, USA). One-hundred micrograms of proteins from skin lysates were used in this study, and 30-kDa Microcon filtration devices (Millipore, Ultracel YM-30, Billerica, MA, USA) were used for detergent removal and protein digestion following filter-aided sample preparation procedures (FASP) [24]. Peptides were eluted from the filter with 0.5 M NaCl. After adjusting the pH of the sample to approximately pH 2–3, the sample was desalted using the C18 spin column (Harvard Apparatus, Holliston, MA, USA) and dried completely using a centrifugal concentrator (SCANVAC, LaboGene Aps, Lynge, Denmark).

2.5. LC–MS analysis for proteomic analysis

Dried peptides were resuspended in 100 μL of water with aqueous 0.1% formic acid (FA) for LC–MS/MS analysis and separated in a capillary column packed with C18 at a flow rate of 0.3 μL/min for min. Mobile phase A (0.1% FA in H_2O) and mobile phase B (90% acetonitrile, 0.1% FA in H_2O) were used to establish the 90-min gradient of 3–45% B (0–60 min), 45–90% B for 60–60.01 min, 90% B for 60.01–75 min, 90–10% B, 75–75.01 min, and 10–3% B for 75.01–90 min. The peptide samples were analyzed by 6550 Accurate-Mass Q-TOF LC/MS (Agilent Technologies, DE, USA) at an electrospray potential of 1.8 kV. A drying gas flow of 11 L/min and a fragmentor at 175 V were used. The Q-TOF was set to perform data

acquisition in the positive mode so an *m/z* range of 100–3000 was used in the MS and MS/MS scan. Each sample was subjected to LC–MS three times for reproducibility.

2.6. Database searching for proteomic analysis

Tandem mass data from the Q-TOF instrument was converted to .mzXML format by Trapper 4.3.1 (TPP, ISB, USA) for database searching in SEQUEST (Sorcerer 3.5; Sage-N Research, Lajolla, CA, USA). Search parameters were as follows: precursor mass tolerance — 20 ppm, product ion mass tolerance — 50 ppm, 2 missed cleavages allowed, fully tryptic peptides only, fixed modification of carbamidomethyl cysteine, variable modifications of oxidized methionine, and N-terminal carbamylation. A criteria probability score of 0.95 was used for this result. This score represents a false positive rate of less than 1% based on PeptideProphet probability criteria. This score was used to evaluate the quality of protein identification with an error rate of less than 5% (about probability value 0.9).

2.7. Label-free quantification by IDEAL-Q for proteomic analysis

For the label free quantification, we use IDEAL-Q software. Input data included database search results and mzXML files, wherein the raw data files from the Agilent Q-Tof mass spectrometer were converted into mzXML format, using Trapper software (Institute for Systems Biology, Seattle, WA, USA). Then an ID database containing the identified peptides and proteins in all the LC–MS/MS runs was constructed. IDEAL-Q was used to sequentially process all the peptides in each LC–MS/MS run, both identified and unidentified, to quantify as many peptides as possible, then the predicted elution time was used to detect peak clusters of the assigned peptide. The detected peptide peaks were processed by statistical and computational methods and further validated by a signal-to-noise (S/N) ratio >3, correct charge state, and isotopic distribution criteria (SCI validation) to filter out noisy data. Based on the peptide ratio distribution, the peptide normalization step could be processed. Protein abundance ratio was determined by the weighted average of non-degenerate peptides.

2.8. Mouse epidermis preparation for targeted metabolite analysis

Ice-cold methanol (1 mL) was added to the epidermal layer from the central dorsal skin (approximately 2 × 2 cm^2), which was then homogenized (30 frequency) three times for 30 min using a mixer mill MM400 (Retsch®, Haan, Germany). The suspension was centrifuged at 4 °C and 20,000 *g* for 3 min and the resulting supernatant (800 μL) was transferred to a 1.5 mL microcentrifuge tube. Dried samples were stored at −80 °C until gas chromatography–time-of-flight MS (GC–TOF-MS). For GC–TOF-MS analysis, the skin extracts were oximated with 50 μL of methoxyamine hydrochloride (20 mg/mL) in pyridine at 30 °C for 90 min. A second derivatizing agent, 50 μL of MSTFA, was added to the mixture and incubated at 37 °C for 30 min. The final concentration of each analyzed sample was 10 mg dry weight of extract/mL.

2.9. GC–TOF-MS analysis for target metabolites related to TCA cycle

A GC–TOF-MS analysis was performed on an Agilent 7890 GC system (Agilent, Atlanta, GA) coupled with a Pegasus® HT TOF-MS (Leco Corp., St. Joseph, MI, USA) using an Agilent 7693 autosampler (Agilent, Atlanta, GA). The system was equipped with a Rtx-5MS column (29.8 m × 0.25 mm i.d., a particle size of 0.25 μm; Restek Corp., Bellefonte, PA, USA). The front inlet and transfer line temperatures were set at 250 °C and 240 °C, respectively. The helium gas flow rate through the column was 1.5 mL/min, and ions were generated by a −70 eV electron impact (EI). The ion source temperature was set at 230 °C, and the mass range was 40–1000 *m/z*. The column temperature was maintained isothermally at 75 °C for 2 min, raised to 300 °C at a rate of 15 °C/min, and then maintained at 300 °C for 3 min. One microliter of reactant was injected into the GC–TOF-MS with a split ratio of 5:1. The corresponding peaks as target metabolites were confirmed in the original chromatogram and were identified either using commercial standard compounds in comparison with the mass spectra and retention time or on the basis of the NIST mass spectral database (National Institute of Standards and Technology; FairCom, Gaithersburg, MD, USA), and our in-house library. Differences were evaluated using Student's *t*-test (for 2 groups) or one-way ANOVA analysis (for 4 groups), using Statistica 7 (StatSoft Inc., Tulsa, OK, USA). The significance of the changes remains clear; significant at $p < 0.05$.

2.10. In vitro experiment

HaCaT human keratinocytes were plated in 100 mm tissue culture dishes and maintained in DMEM supplemented with 10% heat-inactivated FBS and 1% PS at 37 °C in a humidified atmosphere containing 5% CO_2. Cell morphology was confirmed, and senescence-associated β-galactosidase (SA-β-Gal) and senescence-associated heterochromatin foci (SAHF) stainings were performed using poly-L-lysine coated glass coverslips. The poly-L-lysine-coated coverslips were put into a 24-well plate, and then HaCaT (1×10^4 cells/well) cells were seeded onto them. After 24 h, cells were washed twice using phosphate buffered saline (PBS), and 200 μL of PBS was added. The cells were then exposed to UVB irradiation once, and then incubated for 24 h. Control cells were kept in the same culture conditions without the UVB exposure. After washing with PBS, cell morphology was examined with a light microscope. To perform SA-β-Gal staining, the cells were fixed with 4% paraformaldehyde (PFA) at room temperature for 10 min. After two additional washes with PBS, staining solution (Cell Signaling Technology Inc., Danvers, MA, USA) was added to the cells, and they were incubated at 37 °C overnight in a dry incubator (no CO_2). The cells were again washed with PBS and photographed under bright field microscopy to detect blue cells. The number of SA-β-gal positive cells/field was counted in five fields/slide, and the mean number of positive cells/field (magnification, ×200; area, 0.36 mm^2) was calculated. To perform SAHF immunohistochemistry, HaCaT cells were fixed with 4% PFA, and blocked with 1% normal donkey serum at RT. After 1 h, cells were incubated with specific antibodies against trimethyl-Histone H3 (H3K9Me3, heterochromatin

marker, features typically associated with SAHF [25]) for 1 h at 4 °C. Then, the cells were also stained with an Alexa-Fluor® 488 conjugated rabbit polyclonal antibody and a DAPI solution. Finally, the cells were mounted with the VECTASHIELD® mounting media, and visualized using fluorescence microscopy.

For Western blot analysis, HaCaT (5×10^5 cells/well) were seeded in non-coated 6-well plates. After 24 h, the cells were washed twice using PBS, and 500 μL of PBS was added. The HaCaT cells were irradiated with the desired dose of UVB, and then the treated aloe extract (25 μg/mL) and aloesin (1 μM). The cells were harvested 24 h after UVB irradiation.

Normal human dermal fibroblasts (NHDFs) from juvenile foreskin were purchased from PromoCell (Heidelberg, Germany). The cells were maintained in DMEM supplemented with 10% heat-inactivated FBS and 1% PS at 37 °C in a humidified atmosphere containing 5% CO_2 with a media change every other day. Subcultures were conducted with a dilution ratio of 1:4 (volume ratio of mother culture to fresh medium) at 4 day intervals. In this study, we used NHDF with passage numbers until P10 (population doublings; >15). NHDF (1.2×10^5 cells/dish) were seeded in a non-coated 40 mm dish. After 24 h, the cells were washed twice with PBS, and 500 μL of PBS was added. The NHDFs were then irradiated with 144 mJ/cm^2 UVB once. After 72 h, we measured matrix metalloproteinase 1 (MMP-1) and procollagen type 1 (PC-1) levels in the culture medium, and performed Western blot analysis on the cell lysates. This method is commonly used in research on the development of skin anti-photoaging agents by our research group, and had been also published [26].

2.11. Western blot analysis

HaCaT cells and the skin tissues of hairless mice were lysed in cold lysis buffer (50 mM Tris–Cl, pH 8.0, 0.1% sodium dodecyl sulfate (SDS), 150 mM sodium chloride, 1% NP-40, 0.02% sodium azide, 0.5% sodium deoxycholate, 100 μg/mL phenyl methyl sulfonyl fluoride, and 1 μg/mL aprotinin). The extract total protein content was determined using bovine serum albumin as the standard. Fifty μg of proteins was separated by SDS polyacrylamide gel electrophoresis (10% or 15% acrylamide gels) and transferred to a nitrocellulose membrane (Amersham Pharmacia Biotech, Amersham, UK). The membrane was blocked with 5% non-fat skim milk with Tris-buffered saline-T (TBST) and incubated overnight with the primary antibodies of DLD, involucrin (IVN), MMP-1, PC-1 (1:1000 dilution), and α-tubulin (1:3000 dilution) at 4 °C. The membranes were washed three times with TBST and incubated with secondary antibodies for 1 h at room temperature. The membranes were developed using enhanced chemiluminescence reagents (Amersham Pharmacia Biotech).

Band intensities were quantified using NIH Image-J software (Bethesda, MD, USA). The integrated area of each band was normalized to the integrated area of the tubulin band on the same blot (mean of the integrated area of protein in normal mice was indicated as 1). Data represent the means (n = 3). Statistical comparisons between different groups were performed using a Student's *t*-test or a one-way ANOVA test followed by Newman–Keuls multiple range test. $p < 0.05$ indicates statistically significant differences.

2.12. High-performance liquid chromatography analysis

To measure the content of aloesin in the aloe extract, a high-performance liquid chromatography (HPLC) analysis was performed. The analysis was carried out on a Waters system (Waters Corp., Milford, MA, USA) consisting of separation module (e2695) with a photodiode array detector (2998). UV absorbance was monitored from 200 to 500 nm. A qualitative analysis was carried out by 254 nm and column temperature was maintained at 40 °C. Separation was carried out using an YMC-Triart C18 (250 × 4.6 mm; particle size, 5 um; YMC Co. Ltd., Japan). The mobile phase comprised water (solvent A) and acetonitrile (solvent B). The flow rate was 1 mL/min. The gradient was as follows: 0.0 min, 95% A; and 20.0 min, 80% A.

3. Results

3.1. Histological investigation of skin photodamage

Long-term UVB exposure caused photodamage as evidenced by histological and molecular changes in the skin. The UVB exposure leads to increased epidermal thickness for protection against further UVB damages. Moreover, it induces collagen breakdown and decreases collagen synthesis by MMPs activation and PC-1 reduction in the dermis. We confirmed the histological changes and extracellular matrix modulating factors expression in the skin of hairless mice after UVB exposure. Histological changes in the dorsal skin were observed by hematoxylin–eosin and Masson's trichrome stainings. The UVB-irradiated mice had thicker epidermal layers than non-irradiated mice (Fig. 1A). In addition, the collagen fibers of the UVB-irradiated mice were less dense and more erratically arranged compared to the dense, regular fibers of non-irradiated mice (Fig. 1B). Based on the Western blot analysis, PC-1 protein levels decreased while the levels of MMP-1 significantly increased in the dermis of the UVB-exposed hairless mice skin (Fig. 1C). Therefore, the results clearly indicate that skin photoaging and photodamage were successfully induced in our animal experiments.

3.2. Identification of novel UVB target, DLD, in the epidermis using proteomic analysis

For proteomic analysis, epidermal specimens from the normal and UVB-irradiated skin were used, and the LC–MS/MS analysis was performed. In this study, we identified a total of 622 and 638 proteins in the epidermis of the normal and UVB-exposed mice, respectively, at a false discovery rate (FDR) of 1%. Table 1 shows the list of differentially expressed proteins obtained from label-free quantification using IDEAL-Q. For each identified protein, the relative abundance ratio between the UVB-exposed versus normal epidermis was listed with the protein probability score (FDR 1%) and standard deviation value of quantification ratio. Our results found 57 differentially expressed proteins from the dorsal epidermis of the UVB-irradiated mice. Among those, 29 proteins were over-expressed and 28 proteins were down-expressed in the epidermis of the photodamaged skin. The cut-off criteria for the differentially expressed proteins were set with an adjusted ratio of >2.0-fold difference. These

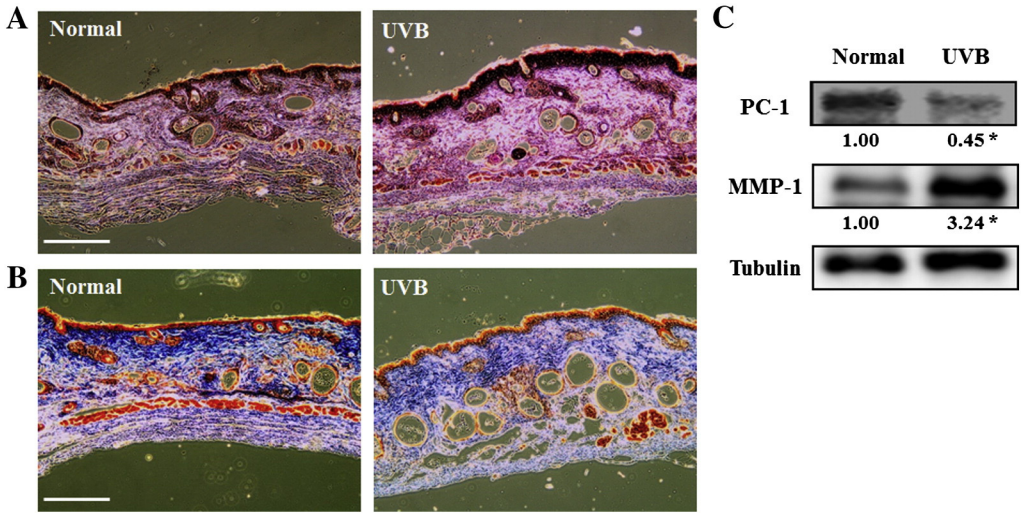

Fig. 1 – Photoaging-associated histological and molecular changes in the skin of UVB-exposed mice. We randomly divided hairless mice into 2 groups: non-UVB exposed (normal), and UVB irradiated groups (UVB). UVB radiation (total dose of 5000 mJ/cm^2) was applied to the dorsal skin of the mice for 4 weeks. To investigate the UVB-induced skin photoaging and photodamage, we confirmed histological changes by (A) hematoxylin–eosin and (B) Masson's trichrome stainings using skin biopsies (scale bar = 1 mm). Moreover, we also performed (C) Western blot analysis for confirmation of PC-1 and MMP-1 expressions in the skin. Band intensities were quantified using NIH Image-J software (Bethesda, MD, USA). The integrated area of each band was normalized to the integrated area of the tubulin band on the same blot (the mean of the integrated area of protein in normal mice was indicated as 1). Data represent the means (n = 3). Statistical comparisons between different groups were performed using a Student's t-test. $^*p < 0.05$ indicates statistically significant differences. PC-1, procollagen type 1; MMP-1, matrix metalloproteinase 1.

differentially expressed proteins were analyzed by Ingenuity Pathway Analysis (IPA) software (Qiagen, Redwood City, CA, USA). IPA software performs comprehensive analysis of proteins and related biological processes according to the proteomic data. Biological functions were imported and scored by most significantly affected processes according to these differentially expressed proteins. Fig. 2 shows that differentially expressed proteins were related to biological functions such as developmental disorders, cellular movement, and cell death and survival due to photodamage.

Previous studies had reported that photodamage and photoaging might be associated with changes in the efficiency of the TCA cycle, a cellular metabolism pathway [27,28]. Therefore, we selected proteins associated with the TCA cycle. In this study, 7 proteins including aconitase 2, citrate synthase, dihydrolipoyl dehydrogenase (DLD), isocitrate dehydrogenase 3, malate dehydrogenase 1 and 2, and oxoglutarate dehydrogenase were identified (Fig. 3). Among these, DLD was the only TCA cycle-associated protein where expression was changed by UVB irradiation. In the epidermis of the UVB irradiation-induced photoaged skin, the DLD expression declined significantly compared to the normal group.

3.3. *Analysis of target metabolites related to the TCA cycle in mouse epidermis*

To investigate the TCA cycle-related metabolites in the epidermis, we performed a target analysis for detecting the intermediates and products of the TCA cycle in the epidermal segments using GC–TOF-MS. As shown in Fig. 3, pyruvate, citric acid, malic acid, and fumaric acid, the TCA cycle-related metabolites, were detected in the epidermal layers from the dorsal skin. The levels of malic acid and fumaric acid were significantly decreased in the UVB-treated group compared to the normal group, whereas there was no difference between the two groups in the levels of pyruvate and citric acid. DLD participates in L-isoleucine degradation [29]. In this study, the level of L-isoleucine was significantly decreased in the epidermis of the UVB-irradiated skin (Fig. 3).

3.4. *Change of the DLD expression in mouse epidermis and HaCaT cells*

To validate DLD as a biomarker, Western blots were performed to detect the DLD expressions levels using skin epidermal fragments. IVN was used as an epidermal specific marker in the granular and spinous layers of the skin [30]. As shown in Fig. 4A, the IVN proteins were strongly detected in both the normal and the UVB-exposed skin. Namely, the results clearly indicate epidermal fragmentation in the skin tissue of hairless mice in this study. The DLD protein levels were significantly decreased in the epidermis of the photodamaged mice in comparison with the normal group. We also confirmed the DLD expression in the mouse epidermis by immunohistochemistry using the DLD-specific antibody. As shown in Fig. 4B, we found a decrease in the DLD expression in the epidermis of the UVB-irradiated mice compared to the normal mice. These data are in agreement with the mass spectrometry data showing a 0.224-fold decrease following the exposure to UVB radiation (Table 1).

Table 1 – List of differentially expressed proteins in the epidermis from mouse dorsal skin tissue identified by LC–MS/MS analysis.

Accession #	Description	Protein score (FDR 1%)	# of peptides	UVB/ normal	SD value
P97351	40S ribomal protein S3a	1	6	2.012	0
Q64727	Vinculin	1	10	53.626	0
P10126	Elongation factor 1-alpha 1	1	14	2.676	0.831
P35173	Stefin-3	1	8	2.286	0.874
Q03265	ATP synthase subunit alpha, mitochondrial	1	23	2.443	7.729
Q921H8	3-Ketoacyl-CoA thiolase A, peroxisomal	1	4	2.154	0
Q9CZU6	Citrate synthase, mitochondrial	1	12	2.449	3.613
Q9D9V3-2	Isoform 2 of ethylmalonyl-CoA decarboxylase	1	6	3.071	0
Q9EPL9	Peroxisomal acyl-coenzyme A oxidase 3	1	2	2.485	0
Q9CRB1	Galectin-7	1	14	2.133	4.195
Q3V2T4-2	Isoform 2 of keratinocyte differentiation-associated protein	1	2	2.83	0
P60766	Cell division control protein 42 homolog	1	4	2.444	0
Q76MZ3	Serine/threonine–protein phosphatase 2A 65 kDa regulatory subunit A alpha isoform	1	7	2.292	4.815
P28656	Nucleome assembly protein 1-like 1	1	2	5.548	0
P11087-2	Isoform 2 of collagen alpha-1(I) chain	1	2	2.982	0
Q9CQ92	Mitochondrial fission 1 protein	1	2	2.024	0
P59325	Eukaryotic translation initiation factor 5	1	2	2.68	0
Q99LC5	Electron transfer flavoprotein subunit alpha, mitochondrial	1	4	2.009	1.513
P10605	Cathepsin B	1	3	12.547	0
O55142	60S ribomal protein L35a	1	5	2.048	0
Q9JHU4	Cytoplasmic dynein 1 heavy chain 1	1	8	2.013	0
P62754	40S ribomal protein S6	1	5	8.134	0
Q9D0I9	Arginine–tRNA ligase, cytoplasmic	0.9942	2	20.918	0
Q9JIF0-2	Isoform 2 of protein arginine N-methyltransferase 1	0.9989	3	35.842	0
P10649	Glutathione S-transferase Mu 1	1	3	106.748	0
Q91VD9	NADH–ubiquinone oxidoreductase 75 kDa subunit, mitochondrial	1	2	2.205	0
P23492	Purine nucleidephosphorylase	1	3	2.001	0
Q6ZWV3	60S ribomal protein L10	1	3	2.13	0
P26516	26S proteasome non-ATPase regulatory subunit 7	1	2	2.168	0
P11352	Glutathione peroxidase 1	1	5	0.374	2.361
Q8VEM8	Phosphate carrier protein, mitochondrial	1	7	0.449	1.387
O70503	Estradiol 17-beta-dehydrogenase 12	1	6	0.271	2.307
P15864	Histone H1.2	1	5	0.365	0
P16546-2	Isoform 2 of spectrin alpha chain, non-erythrocytic 1	1	18	0.396	1.393
P17751	Triephosphateisomerase	1	11	0.287	4.462
E9QPZ3	Filaggrin-2	1	9	0.359	1.367
Q6ZWZ6	40S ribomal protein S12	1	4	0.48	0
P02301	Histone H3.3C	1	3	0.455	0
P62301	40S ribomal protein S13	1	5	0.496	1.562
P26369	Splicing factor U2AF 65 kDa subunit	1	2	0.351	0
P08207	Protein S100-A10	0.9941	2	0.487	0
A2A863-2	Isoform 2 of integrin beta-4	1	6	0.489	1.455
Q8R081	Heterogeneous nuclear ribonucleoprotein L	1	2	0.437	0
P02088	Hemoglobin subunit beta-1	1	9	0.27	1.33
Q9CZM2	60S ribomal protein L15	0.9998	4	0.376	0
O08749	Dihydrolipoyl dehydrogenase, mitochondrial	1	2	0.224	0
Q9D952	Envoplakin	1	5	0.487	0
Q8BWT1	3-Ketoacyl-CoA thiolase, mitochondrial	1	2	0.482	0
P62843	40S ribomal protein S15	1	2	0.439	0
Q61166	Microtubule-associated protein RP/EB family member 1	0.9999	3	0.178	0
O08997	Copper transport protein ATOX1	0.9763	2	0.293	0
P42227-2	Isoform Stat3B of signal transducer and activator of transcription 3	0.9081	2	0.257	0
Q9CQF9	Prenylcysteine oxidase	0.986	2	0.466	0
Q91X72	Hemopexin	1	3	0.405	0
Q9Z0N1	Eukaryotic translation initiation factor 2 subunit 3, X-linked	0.9376	2	0.206	0
Q61496	Probable ATP-dependent RNA helicase DDX4	0.9132	2	0.108	0
E9Q4Y1	Protein Adh6a	1	4	0.483	0

The main cell type in the epidermis is the keratinocyte. Therefore, to confirm the change in the DLD expression in the UVB-damaged epidermis, we also used the human keratinocyte cell line, HaCaT. As expected, the DLD protein expression was significantly reduced in the UVB-exposed HaCaT as seen in Fig. 4C. Moreover, the cells showed a flattened morphology and

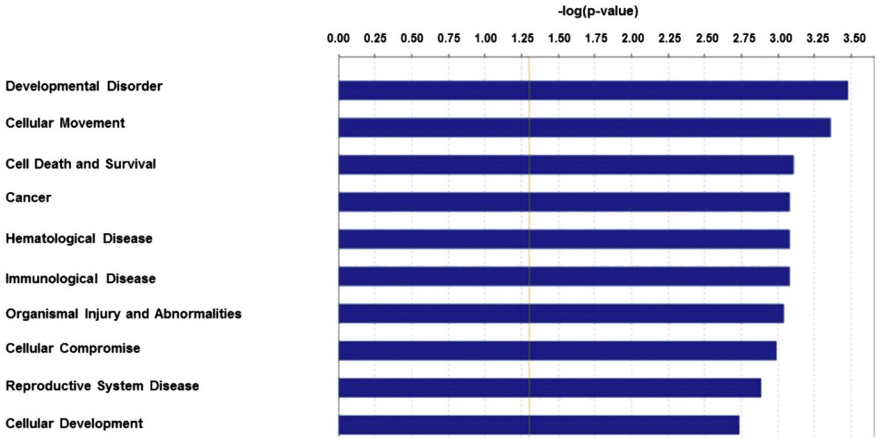

Fig. 2 – Rank of diseases and biological functions related to differentially expressed proteins. These proteins were imported and scored by IPA software of diseases and biological function database. Statistical analysis was utilized by *t*-test and the *p*-value was obtained. These biological functions have reliable *p*-values above the calculated threshold. Photodamage affects the expression of numerous proteins related to cell death, survival, and development.

we observed a progressive retraction of the cell body with small blebs following the exposure to UVB at doses of 100 mJ/cm^2 (Fig. S4A). These changes are representative morphological features of the aged cells. This result was consistent with previous results published by Giacomoni [76]. SA-β-Gal and SAHF are widely used as biomarkers of senescent and aging

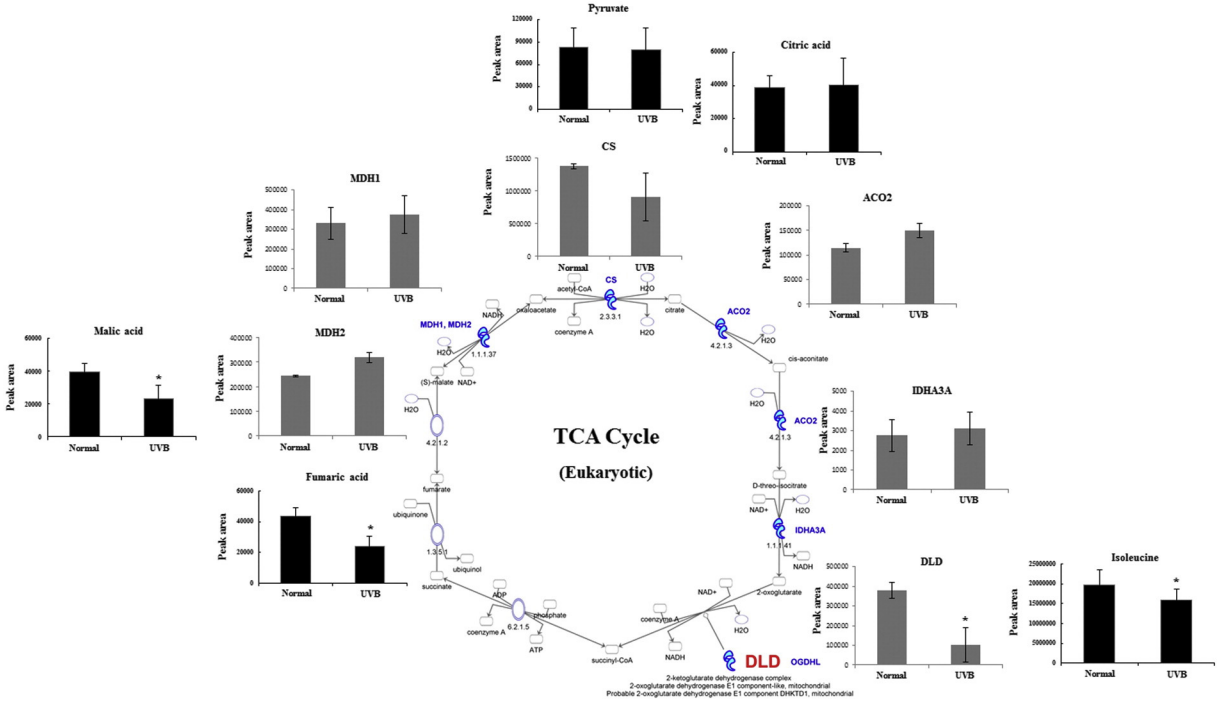

Fig. 3 – The proposed TCA cycle pathway from the identified proteins and metabolites in the epidermis of normal and UVB-exposed mice. Proteomes of the epidermal segments were analyzed using Q-TOF LC–MS system, and database searching and label-free quantification were performed through SEQUEST and IDEAL-Q software, respectively. Metabolites were analyzed by GC–TOF-MS. The corresponding peaks as target metabolites were confirmed in the original chromatogram and were identified either using commercial standard compounds for comparing the mass spectra and retention times or on the basis of the NIST mass spectral database and our in-house library. The peak area plotted on the Y-axis represents the peak area of identified ion MS fragment (*m*/*z*) of each protein and metabolite in total ion chromatogram (TIC).ACO_2, aconitase2, mitochondrial; CS, citrate synthase; DLD, dihydrolipoyl dehydrogenase; IDH3A, isocitrate dehydrogenase 3 (NAD^+) alpha; MDH1, malate dehydrogenase 1, NAD (soluble); MDH2, malate dehydrogenase 2, NAD (mitochondrial); and OGDH, oxoglutarate (alpha-ketoglutarate) dehydrogenase (lipoamide).

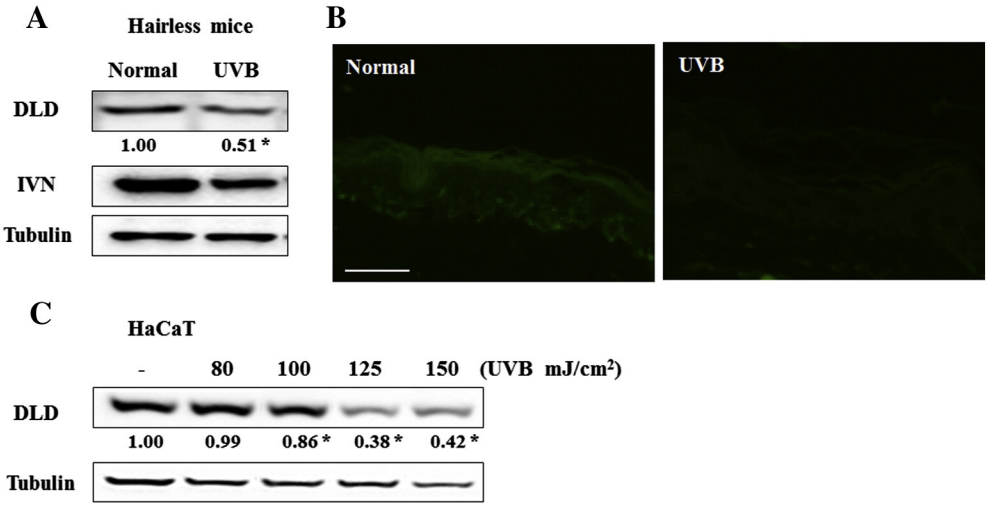

Fig. 4 – Validations of DLD in the skin epidermal segments by Western blot analysis and immunohistochemistry. DLD protein expressions were determined by (A) Western blot analysis and (B) immunohistochemistry using a DLD-specific antibody in the epidermal segments of hairless mice skin. In this study, IVN was used as an epidermal specific marker. House-keeping tubulin protein levels are also shown. Skin tissue was stained with Alexa Fluor® 488 conjugated rabbit polyclonal antibody (scale bar = 10 μm). (C) To confirm the change in the DLD expression in UVB-damaged epidermis, we also used the human keratinocyte cell line, HaCaT, and performed Western blot analysis. The integrated area of each band was normalized to the integrated area of the tubulin band on the same blot (the mean of the integrated area of protein in normal mice was indicated as 1). Data represent the means (n = 3). Statistical comparisons between different groups were performed using a Student's *t*-test. *$p < 0.05$ indicates statistically significant differences.

cells. In particular, SA-β-Gal is overexpressed and accumulates in both keratinocytes and fibroblasts following the UVB exposure [31,32]. Therefore, we performed SA-β-Gal and SAHF stainings in HaCaT. As shown in Fig. S4B, as expected, the UVB irradiation led to an increase in the number of SA-β-Gal-positive cells. However, the percentages and the proportions of the SAHF-positive calls did not change by the UVB irradiation (Fig. S4C). These results indicate that our in vitro experimental condition did not influence the SAHF accumulation in the HaCaT cells, and that measurement of SA-β-Gal activity may be more suitable for detecting photoaging than confirmation of SAHF accumulation.

3.5. Change of the DLD expression in mouse dermis and NHDF

Although our investigation was focused only on the epidermal skin and keratinocyte cell line, the skin is composed of different layers and cell types containing fibroblasts. Dermal fibroblasts, in particular, are the major source of MMPs that are expressed in response to the UV irradiation and provoke collagen degradation [33,34]. The fibroblasts are also an established model for cellular senescence. Therefore, we investigated whether the DLD expression levels also declined in dermal fibroblast following UVB irradiation. As shown in Fig. S8, as expected, the UVB irradiation increased the PC-1 levels and decreased the MMP-1 levels in the NHDF cells. However, the DLD expression was not decreased by UVB in the NHDF cells. Moreover, no significant change was observed in the DLD expression in the dermis of the photoaged hairless mice. The decrease in the DLD expression due to the UVB-induced photoaging may therefore be a more specific phenomenon in the epidermis and keratinocyte cells than in the dermis and fibroblast cells.

3.6. Application of novel UVB targets in *A. vera*-treated photoaged skin

Previously, we reported on the in vitro anti-photoaging effects of *A. vera* [26]. Therefore, to investigate the effects of aloe on skin photoaging in vivo, topical applications of the aloe extract were applied three times a week for 3 weeks on the dorsal skin of the UVB-irradiated hairless mice. As shown in Fig. 5A, the UVB-induced increase in the epidermal thickness and the decrease in dermal collagen density were recovered by aloe treatment. Moreover, the aloe treatment increased PC-1 protein levels, and inhibited MMP-1 expression in the dermis (Fig. 5B). Based on our study, aloe was more effective than retinyl palmitate, a popular cosmeceutical. Therefore, these results support that the *A. vera* extract may be a potential anti-photoaging agent.

To underscore the importance of these novel UVB targets, DLD, malic acid, and fumaric acid, we used skin tissue treated topically with *A. vera* extract and performed Western blot, proteomic, and targeted metabolite analyses. As shown in Fig. 5B, the aloe-treated group had a significant increase in the protein expressions of IVN and DLD in the epidermal fragments. This result was similar to that from our proteomic analysis (Fig. 5C). In HaCaT cells, the UVB-induced decrease in the DLD expression was also prevented by treatment with aloe extract and its active compound, aloesin (Fig. S5). As shown in Fig. S5B, aloesin increased the DLD protein levels at only 1 μM. At the other concentrations (0.01 and 0.1 μM), aloesin did not influence the DLD expression. Aloesin did not show dose-dependent effects under our experimental conditions. These results were similar to those of our previous study [26], where aloesin's effect on an increase in PC-1 mRNA

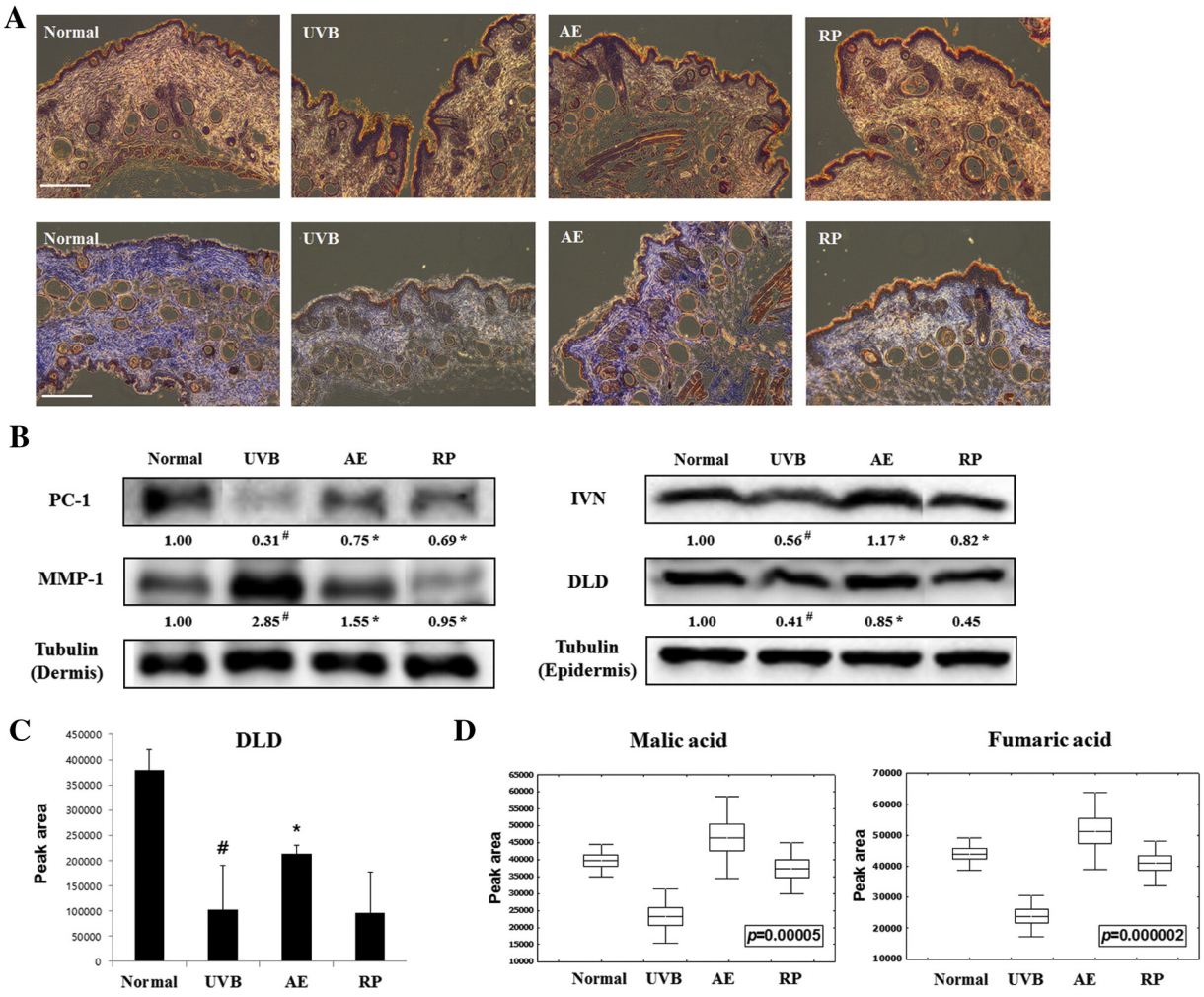

Fig. 5 – Application of novel UVB targets in aloe-treated photoaged skin. We randomly divided hairless mice into 4 groups: non-UVB exposed (normal), UVB irradiated groups (UVB), UVB + aloe extract-treated (AE), and UVB + retinyl palmitate-treated (RP) groups. UVB radiation (total dose of 5000 mJ/cm^2) and topical application of aloe extract (for 3 weeks) were applied to the dorsal skin of the mice. To investigate the effects of aloe extract on UVB-induced skin photodamaged and photoaging, we confirmed histological changes by (A) hematoxylin–eosin (upper layer) and Masson's trichrome stainings (lower layer) using skin biopsies (scale bar = 1 mm). We also performed (B) Western blot analysis for confirmation of PC-1 and MMP-1 in the dermis, IVN and DLD in the epidermis, and (C) proteomic analysis of DLD protein levels in the epidermis of hairless mice skin (each # and *indicate statistically significant differences [$p < 0.05$] compared to the normal and UVB groups). (D) Moreover, metabolite analysis of malic acid and fumaric acid were performed using epidermal fragments. PC-1, procollagen type 1; MMP-1, matrix metalloproteinase 1; IVN, involucrin; DLD, dihydrolipoyl dehydrogenase.

expression was not dose-independent in the UVB-irradiated human dermal fibroblasts. To measure the content of aloesin in the aloe extract, an HPLC analysis was performed. Fig. S12 shows a chromatogram obtained for the aloesin and aloe extract. The calibration curve of the aloesin showed a good linearity and correlation coefficient is 0.9916. The aloesin content in the aloe extract is 0.124 ± 0.004 μg/mg based on our HPLC analysis.

The UVB-induced decrease in the levels of malic acid and fumaric acid was also recovered by the aloe treatment in the epidermis (Fig. 5D). These results strongly indicate that novel UVB targets in the epidermis, DLD, malic acid and fumaric acid, can be available for the development of cosmeceuticals and nutraceuticals, thus regulating the changes induced from skin photodamage and photoaging.

4. Discussion

The skin photobiology of photoaging is not yet fully understood, although its clinical importance has increased. A new biomarker has yet to be found for skin photoaging and skin photodamage, especially candidates that can be used to diagnose, prevent, and treat skin photodamage. The aim of this study was to try to find a clinically meaningful novel biomarker for skin photoaging. Currently, photodamage can be characterized as changes in skin barrier function, hydration and skin turnover, as well as the smoothness and depth of wrinkles. The photoaged or UVB damaged skin is usually diagnosed by visual detection of changes in lines and

wrinkles, pigmentation, elasticity, firmness etc. However, these general markers can be affected by extrinsic risk factors such as not only UVRs but also intrinsic risk factors such as hormone deficiency. Therefore, our study was focused on identifying a biomarker that could be used in practice for the diagnosis of UVB damaged skin induced only by the UVB overexposure. We thought that finding a biomarker that provokes the changes in skin phenotype is important. This study is intended to find a new biomarker of skin photodamage using the UVB-irradiated hairless mice through the integration of proteomics and targeted metabolite analysis. This study focused only on the dorsal epidermal skin from the UVB-exposed hairless mice because the epidermis is the signaling interface between the organism and the environment and protects against harmful stimuli such as UVB [4]. In this study, we identified 622 and 638 expressed proteins in the epidermis of the normal and the UVB-exposed mice using the LC–MS-based proteomic analysis, respectively. We investigated the biological functions of the differentially expressed proteins by IPA software. These proteins were highly related to developmental disorders, cellular movement, and cell death and survival. We proposed that the differentially expressed proteins have roles in changing cellular states in the epidermal tissue. Aging and many pathological processes in somatic cells have been known to be associated with the alteration of energy metabolism as a result of mitochondrial damages such as oxidative stress [35–37]. The TCA cycle is an essential metabolic network, which generates energy via a supply of precursors for anabolic processes and reducing factors [38]. Therefore, we first selected 7 proteins associated with the TCA cycle that are essential for metabolism. In this study, DLD was the only protein that changed after the UVB exposure among the TCA cycle-associated proteins. In the UVB-irradiated epidermis, the DLD expression declined significantly compared to the normal. Therefore, we selected the DLD as a potential biomarker candidate of skin photoaging and photodamage. Little is known of the relationship between protein and metabolite levels due to physiological responses to the UVB exposure. Some metabolites may represent the end-point of the biochemical processes in the epidermis. Therefore, we performed the targeted metabolite analysis to investigate whether the decrease of the DLD protein expression in photodamaged epidermis is related to the change in the levels of TCA cycle metabolites. We analyzed the TCA cycle-associated metabolites using GC–TOF-MS, and identified 2 differentially synthesized metabolites, malic acid and fumaric acid. These are not direct metabolites of DLD during the TCA cycle. Direct metabolites such as dihydrolipoamide, lipoamide, 2-oxoglutarate, succinyl-CoA, acetyl CoA, 2-oxoisovalerate and isobutanoyl-CoA, were not detected in this study. Therefore, we suggest that the decrease of the DLD protein expression in photoaged skin may not directly influence the metabolites. Namely, it may have an effect on the metabolites through a series of subsequent enzymes such as succinate dehydrogenase, fumarase, and malate dehydrogenase. In other words, the decline of the DLD protein expression may induce the alteration of the TCA cycle function in photoaged skin. Moreover, we have shown that the integration of proteomic and targeted metabolite analyses can be used for the discovery of novel biomarkers.

Unfortunately, this study did not include the data of a group without vehicle treatment that represent the true meaning of normal skin. However, you can refer to our previous study published in Metabolomics in Aug 2014 [77]. As previous researches, we used same mouse strain, SKH-1 (6-week, female), and exposed the dorsal skin to UVB for 6 and 12 weeks. During that animal experiment, no applications were made to the skin. We then analyzed the skin specimens using MS-based metabolomics. Our metabolite profiling revealed normal skin metabolites as well as time-dependent skin biomarkers (ceramide, *cis*-urocanic acid, and lysophospholipid, etc.) in mice subjected to prolonged chronic exposure to UVB. In the investigation, we also found that the levels of the TCA cycle-associated metabolites (fumaric acid and citric acid) were changed by long-term UVB irradiation.

Oxidative damage in the mitochondria by reactive oxygen species (ROS) overproduction is one of the main signals of the photoaged skin. Because mitochondria are the cellular engines responsible for generating high energy, aging is associated with the alteration of energy metabolism. Moreover, under oxidative stress conditions, mitochondria act not only as targets but also as producers of ROS, which can attack numerous mitochondrial proteins [39]. Cellular processes associated with energy metabolism can be divided into three stages: (1) glycolysis, (2) TCA cycle, and (3) electron transport chain. Among them, the TCA cycle and electron transport chain occur in the mitochondria while glycolysis occurs in the cytoplasm. Previously, it was shown that the mitochondrial electron transport chain activity declined in the photodamaged and chronologically aged skin [40,41]. However, the molecular and functional changes of the TCA cycle, the central metabolic hub of the cells, in photoaged skin have not been reported yet. A previous study reported that deletions or mutations in the mitochondrial DNA were induced by photodamage rather than chronologic aging in human skin [42]. Moreover, Puntel et al. also showed that the antioxidant properties of the TCA cycle protected against malonate pro-oxidant activity in vitro [43]. Therefore, we focused on the possibility of a shift in the TCA cycle due to UVB radiation. In this study, we confirmed that only DLD changed the expression with UVB exposure. The DLD is a flavoprotein enzyme that catalyzes the NAD^+-dependent oxidation of dihydrolipoamide into lipoamide, which belongs to the pyridine nucleotide–disulfide oxidoreductase family [44]. It was already reported that DLD plays a role in cellular defense against lipid oxidation [45–47]. It is the integral component (E_3) of the metabolic multi-enzyme complexes, including pyruvate dehydrogenase, α-ketoglutarate dehydrogenase, and the branched-chain α-keto acid dehydrogenase [48]. In particular, α-ketoglutarate dehydrogenase can be a crucial target of ROS and regulate the deficit of mitochondrial metabolism with oxidative stress [49]. Moreover, DLD has been known to be inactivated by ROS [39]. However, the E_3 components of both α-ketoglutarate dehydrogenase and pyruvate dehydrogenase complexes appear to be the principal ROS source generating O_2^-. and H_2O_2 [50–52]. In other words, DLD may act not only as the ROS target but also as the ROS source, and the decrease of the DLD expression in the epidermis of the photoaged skin may be associated with oxidative stress in the mitochondria. Namely, the biological main function of the UVB-targeted DLD in the skin may be an antioxidant activity, meaning that DLD can help protect against skin tissue damage due to the UVB-induced oxidative stress.

As mentioned above, DLD plays a role in mitochondrial energy metabolism and cellular defense against oxidative stress. Therefore, it can affect the regulation of lactic acidosis and dermatological deterioration due to sensitivity of the dermatological system to defects in oxidative metabolism. Thus, the decrease of DLD may contribute to the increase in oxidative damage, reduction in energy metabolism, and regulation of Fe metabolism and metabolic acidosis. Therefore, the regulation of DLD can be an important target for skin photodamage.

DLD converts dihydrolipoic acid into α-lipoic acid in the cells [53,54]. Interestingly, α-lipoic acid can activate two major regulators of cytoprotective responses to oxidative stress, nuclear factor (erythroid-derived 2)-like 2 (Nrf2) and heme oxygenase-1 (HO-1) [55–58]. Moreover, some findings suggest that α-lipoic acid may have a therapeutic and anti-aging effect through the modulation of the antioxidant status in the aged cells [58–60]. Therefore, it is meaningful that our result may indirectly support the possibility that α-lipoic acid protects against oxidative stress in skin photodamage. In the present study, the DLD protein levels were decreased in the epidermal skin following the UVB exposure. The DLD expression was recovered by treatment with aloe and aloesin in our data. Therefore, our findings support the contention that aloe and aloesin improve the antioxidant capacity of the cells themselves.

In many ways, DLD may correlate with heat burn by irradiation through the overexposure of UVB. Lactic acidosis may be induced by heat burn. It has been found that lactic acidosis developed in severely burned patients [61]. Moreover, DLD can affect the regulation of lactic acidosis at a very early stage [62,63]. Therefore, we think that additional research is needed on the effect of DLD on heat burn due to UVB overexposure.

The DLD activity has been known to be abnormal in the fibroblasts of the patients with Reye-like syndrome and Leigh syndrome [64,65]. However, the functions and precise mechanisms of DLD in the epidermis had not been reported yet. Therefore, this is the first attempt to investigate the role of DLD in the TCA cycle and its related signaling pathway in the photodamaged epidermis. Moreover, we can assert that DLD is a potential biomarker candidate of the photodamaged and photoaged epidermis. And, some biomarkers for the early detection of the acute skin damage by UVB irradiation might be *cis*-urocanic acid [66], cyclobutane pyrimidine dimers (CPDs), pyrimidine (6–4) and pyrimidone photodimers [67]. Our results suggest that DLD may be a potential biomarker that undergoes changes at a later time.

DLD is involved in the TCA cycle but also in isoleucine degradation, the function of the 2-ketoglutarate dehydrogenase complex, and ubiquinol-10 biosynthesis. In this study, several proteins associated with these three pathways were detected (Fig. S6). Among these, a statistically significant difference was found between the normal and UVB groups. We therefore graphed the peak areas of these proteins. The IPA analysis data in Fig. S6 shows that most proteins tended to be upregulated in the epidermal skin following the UVB irradiation. Moreover, DLD also participates in glycolysis and gluconeogenesis. As shown in Fig. S7, triosephosphate isomerase 1 was the only protein associated with glycolysis and gluconeogenesis detected other than DLD. The protein level of triosephosphate isomerase 1 was not changed by the UVB exposure of the epidermal skin of hairless mice. Taken together, the decrease in the DLD level in the skin epidermis was highly significant. This phenomenon in the UVB-induced photoaged epidermal skin is very unique and interesting.

In this study, DLD was identified in the epidermal skin, and decreased DLD protein levels were observed in the UVB-irradiated photoaged skin. Therefore, we concluded that the reduction of DLD may be a biomarker of skin photoaging in the epidermis. However, the possibility cannot be ruled out that the DLD protein expression is also affected by intrinsic factors, particularly chronological aging. Chronological aging has been known to be caused by damage to macromolecules by ROS produced in the mitochondria [68]. Because DLD may act not only as the ROS target, but also as the ROS source [39,49,50,52,69], it is possible that the DLD protein expression can be affected by chronological aging. However, as stated in the manuscript, deletions or mutations in mitochondrial DNA are more frequently induced by photodamage rather than chronological aging in the human skin [42]. The UVB-induced ROS can cause mitochondrial DNA damage, which serves as an important marker of the photoaged skin [70]. Therefore, we hypothesize that reduced DLD expression may be a more specific phenomenon in the photoaged skin than in the chronologically aged skin. Of course, we are not sure that the DLD expression is totally unaffected by chronological aging, as there is insufficient evidence to support this contention. Now, additional in vivo studies are ongoing to determine whether changes in the DLD protein expression occur in the chronologically aged skin (19-month-old mice) compared with young skin (6-week-old mice).

A. vera is one of the most widely used substances in cosmetics. Previously, we reported on its anti-photoaging effects [26]. In this study, we also confirmed that topical application of the aloe extract significantly increases the levels of DLD, malic acid and fumaric acid in the epidermis compared to the UVB-induced photoaged skin. We also focused on aloesin, a C-glycosylated chromone derivative, as a potential active constituent of *A. vera*. It had been reported that aloesin showed various biological properties such as hypopigmentation [71], anti-inflammation [72], and especially antioxidant activities such as free radical scavenging [73]. The improving effects of aloesin on the skin function were also well-known. In particular, the skin-whitening activities of aloesin had been reported in many published data [71,74,75]. Previously, we also reported the inhibitory effect on the skin photoaging of *A. vera* containing aloesin [26], where aloesin treatment increased PC-1 mRNA expression in the UVB-irradiated NHDF. In this study, not only aloe extract but also aloesin treatment increased the DLD expression in the UVB-exposed HaCaT cells. Therefore, we suggest that aloesin may be one of the active ingredients from *A. vera* that ameliorates skin photodamage by promoting an increase in the DLD expression. In our opinion, to determine whether this is in fact the most active compound from aloe extracts, further studies using aloesin-treated photoaged animals and activity-guided isolation techniques in skin-derived cell lines are needed.

We performed an animal study to confirm whether the levels of DLD, malic acid, and fumaric acid were also changed by long-term UVB irradiation. The hairless mice were exposed to the UVB radiation (100 mJ/cm^2 in the first week, 200 mJ/cm^2 in the second week, and 300 mJ/cm^2 in the third week) three times a week for the first 3 weeks. Then, 400 mJ/cm^2 of UVB

was applied three times a week for 9 weeks. First, we confirmed the DLD expression levels in the epidermal skin by Western blot analysis. As shown in Fig. S11, the DLD level was not changed by long-term UVB exposure. This result indicates that the DLD reduction may be a more specific phenomenon in the early stage than in the late stage of skin photoaging. The expression changes of DLD in skin aging with time, in particular, have not yet been reported.

Our results suggest novel UVB targets, as derived from our integration of the proteomic and targeted metabolite analyses, which can be effectively used as biomarkers of photoaging in vivo. Thus, these targets may be used to accelerate the development of novel cosmetic agents that have a beneficial impact on skin photoaging and photodamage.

5. Conclusion

Our strategy to integrate the proteome and targeted metabolites for novel UVB targets is novel. Understanding the integration of the dual data helped draw out strong biomarker candidates in the photodamaged and photoaged skin models. Namely, the proteomics data showed that there was a decrease of DLD in the TCA cycle in the epidermis of the UVB-induced photoaged mice and human keratinocyte cells. In addition, we did a GC–TOF-MS analysis for the target metabolites related to DLD in the TCA cycle. As a result, malic acid and fumaric acid levels were significantly decreased in the epidermis of the UVB-treated mice. These results support that the regulation of the TCA cycle via the decrease of DLD is closely related to the malic acid and fumaric acid metabolites in the epidermis of the UVB-induced photodamage in mice. Furthermore, DLD, malic acid, and fumaric acid can be used for the development of cosmeceuticals and nutraceuticals regulating the change of skin metabolism induced by UVB overexposure.

Our integration of the proteomic and targeted metabolite analytic approach will lead to a better understanding of the unidentified photobiological results from the UVB-irradiated models and can elicit new diagnostic and treatment strategies based on altered metabolism. Application of dual 'omics' for the discovery of biomarkers of skin photoaging is both promising and challenging. Furthermore, our study is the first example of an integration of the proteomic and targeted metabolite analysis techniques to find new biomarker candidates for the regulation of the UVB-induced skin photoaging and photodamages.

Supplementary data to this article can be found online at http://dx.doi.org/10.1016/j.jprot.2014.12.016.

Conflict of interest

The authors state no conflict of interest.

Acknowledgment

This study was supported by a grant of the Korean Health Technology R&D Project, Ministry of Health & Welfare, Republic of Korea (Grant No. HN10C0017).

REFERENCES

[1] Battie C, Verschoore M. Cutaneous solar ultraviolet exposure and clinical aspects of photodamage. Indian J Dermatol Venereol Leprol 2012;78(Suppl. 1):S9–S14.
[2] Armstrong BK, Kricker A. The epidemiology of UV induced skin cancer. J Photochem Photobiol B 2001;63:8–18.
[3] Rabe JH, Mamelak AJ, McElgunn PJ, Morison WL, Sauder DN. Photoaging: mechanisms and repair. J Am Acad Dermatol 2006;55:1–19.
[4] Jansen BJ, Schalkwijk J. Transcriptomics and proteomics of human skin. Brief Funct Genomic Proteomic 2003;1:326–41.
[5] Huang CM, Elmets CA, van Kampen KR, Desilva TS, Barnes S, Kim H, et al. Prospective highlights of functional skin proteomics. Mass Spectrom Rev 2005;24:647–60.
[6] List EO, Berryman DE, Palmer AJ, Qiu L, Sankaran S, Kohn DT, et al. Analysis of mouse skin reveals proteins that are altered in a diet-induced diabetic state: a new method for detection of type 2 diabetes. Proteomics 2007;7:1140–9.
[7] Millioni R, Iori E, Puricelli L, Arrigoni G, Vedovato M, Trevisan R, et al. Abnormal cytoskeletal protein expression in cultured skin fibroblasts from type 1 diabetes mellitus patients with nephropathy: a proteomic approach. Proteomics Clin Appl 2008;2:492–503.
[8] Hensbergen P, Alewijnse A, Kempenaar J, van der Schors RC, Balog CA, Deelder A, et al. Proteomic profiling identifies an UV-induced activation of cofilin-1 and destrin in human epidermis. J Invest Dermatol 2005;124:818–24.
[9] Lamore SD, Qiao S, Horn D, Wondrak GT. Proteomic identification of cathepsin B and nucleophosmin as novel UVA-targets in human skin fibroblasts. Photochem Photobiol 2010;86:1307–17.
[10] Yan Y, Xu H, Peng S, Zhao W, Wang B. Proteome analysis of ultraviolet-B-induced protein expression in vitro human dermal fibroblasts. Photodermatol Photoimmunol Photomed 2010;26:318–26.
[11] Fedele TA, Galdos-Riveros AC, Jose de Farias e Melo H, Magalhaes A, Maria DA. Prognostic relationship of metabolic profile obtained of melanoma B16F10. Biomed Pharmacother 2013;67:146–56.
[12] Hu ZP, Kim YM, Sowa MB, Robinson RJ, Gao X, Metz TO, et al. Metabolomic response of human skin tissue to low dose ionizing radiation. Mol Biosyst 2012;8:1979–86.
[13] Abaffy T, Moller MG, Riemer DD, Milikowski C, Defazio RA. Comparative analysis of volatile metabolomics signals from melanoma and benign skin: a pilot study. Metabolomics 2013;9:998–1008.
[14] Kimball AB. A new era in skin care: the omics revolution. Br J Dermatol 2012;166(Suppl. 2):iii–iv.
[15] Oh JH, Kim YK, Jung JY, Shin JE, Kim KH, Cho KH, et al. Intrinsic aging- and photoaging-dependent level changes of glycosaminoglycans and their correlation with water content in human skin. J Dermatol Sci 2011;62:192–201.
[16] Cozzi SJ, Ogbourne SM, James C, Rebel HG, de Gruijl FR, Ferguson B, et al. Ingenol mebutate field-directed treatment of UVB-damaged skin reduces lesion formation and removes mutant p53 patches. J Invest Dermatol 2012;132:1263–71.
[17] Lee TH, Do MH, Oh YL, Cho DW, Kim SH, Kim SY. Dietary fermented soybean suppresses UVB-induced skin inflammation in hairless mice via regulation of the MAPK signaling pathway. J Agric Food Chem 2014;62:8962–72.
[18] Hwang E, Lee DG, Park SH, Oh MS, Kim SY. Coriander leaf extract exerts antioxidant activity and protects against UVB-induced photoaging of skin by regulation of procollagen type I and MMP-1 expression. J Med Food 2014;17:985–95.

[19] Kang TH, Park HM, Kim YB, Kim H, Kim N, Do JH, et al. Effects of red ginseng extract on UVB irradiation-induced skin aging in hairless mice. J Ethnopharmacol 2009;123:446–51.
[20] Halin C, Fahrngruber H, Meingassner JG, Bold G, Littlewood-Evans A, Stuetz A, et al. Inhibition of chronic and acute skin inflammation by treatment with a vascular endothelial growth factor receptor tyrosine kinase inhibitor. Am J Pathol 2008;173:265–77.
[21] Son ED, Choi GH, Kim H, Lee B, Chang IS, Hwang JS. Alpha-ketoglutarate stimulates procollagen production in cultured human dermal fibroblasts, and decreases UVB-induced wrinkle formation following topical application on the dorsal skin of hairless mice. Biol Pharm Bull 2007;30:1395–9.
[22] Son ED, Lee JY, Lee S, Kim MS, Lee BG, Chang IS, et al. Topical application of 17beta-estradiol increases extracellular matrix protein synthesis by stimulating tgf-Beta signaling in aged human skin in vivo. J Invest Dermatol 2005;124:1149–61.
[23] Begcevic I, Kosanam H, Martinez-Morillo E, Dimitromanolakis A, Diamandis P, Kuzmanov U, et al. Semiquantitative proteomic analysis of human hippocampal tissues from Alzheimer's disease and age-matched control brains. Clin Proteomics 2013;10:5.
[24] Wisniewski JR, Zougman A, Nagaraj N, Mann M. Universal sample preparation method for proteome analysis. Nat Methods 2009;6:359–62.
[25] Narita M, Nunez S, Heard E, Lin AW, Hearn SA, Spector DL, et al. Rb-mediated heterochromatin formation and silencing of E2F target genes during cellular senescence. Cell 2003;113:703–16.
[26] Hwang E, Kim SH, Lee S, Lee CH, Do SG, Kim J, et al. A comparative study of baby immature and adult shoots of *Aloe vera* on UVB-induced skin photoaging in vitro. Phytother Res 2013;27:1874–82.
[27] Yarian CS, Sohal RS. In the aging housefly aconitase is the only citric acid cycle enzyme to decline significantly. J Bioenerg Biomembr 2005;37:91–6.
[28] Fleming SE, Kight CE. The TCA cycle as an oxidative and synthetic pathway is suppressed with aging in jejunal epithelial cells. Can J Physiol Pharmacol 1994;72:266–74.
[29] Sprusansky O, Stirrett K, Skinner D, Denoya C, Westpheling J. The bkdR gene of *Streptomyces coelicolor* is required for morphogenesis and antibiotic production and encodes a transcriptional regulator of a branched-chain amino acid dehydrogenase complex. J Bacteriol 2005;187:664–71.
[30] Eckert RL, Welter JF. Epidermal keratinocytes — genes and their regulation. Cell Death Differ 1996;3:373–83.
[31] Zhang JA, Yin Z, Ma LW, Yin ZQ, Hu YY, Xu Y, et al. The protective effect of baicalin against UVB irradiation induced photoaging: an in vitro and in vivo study. PLoS One 2014;9:e99703.
[32] Bertrand-Vallery V, Boilan E, Ninane N, Demazy C, Friguet B, Toussaint O, et al. Repeated exposures to UVB induce differentiation rather than senescence of human keratinocytes lacking p16(INK-4A). Biogerontology 2010;11:167–81.
[33] Fagot D, Asselineau D, Bernerd F. Matrix metalloproteinase-1 production observed after solar-simulated radiation exposure is assumed by dermal fibroblasts but involves a paracrine activation through epidermal keratinocytes. Photochem Photobiol 2004;79:499–505.
[34] Fagot D, Asselineau D, Bernerd F. Direct role of human dermal fibroblasts and indirect participation of epidermal keratinocytes in MMP-1 production after UV-B irradiation. Arch Dermatol Res 2002;293:576–83.
[35] Bratic I, Trifunovic A. Mitochondrial energy metabolism and ageing. Biochim Biophys Acta 2010;1797:961–7.
[36] Stadtman ER. Role of oxidant species in aging. Curr Med Chem 2004;11:1105–12.
[37] Goldstein S, Ballantyne SR, Robson AL, Moerman EJ. Energy metabolism in cultured human fibroblasts during aging in vitro. J Cell Physiol 1982;112:419–24.
[38] Mailloux RJ, Beriault R, Lemire J, Singh R, Chenier DR, Hamel RD, et al. The tricarboxylic acid cycle, an ancient metabolic network with a novel twist. PLoS One 2007;2:e690.
[39] Yan LJ, Sumien N, Thangthaeng N, Forster MJ. Reversible inactivation of dihydrolipoamide dehydrogenase by mitochondrial hydrogen peroxide. Free Radic Res 2013;47:123–33.
[40] Krutmann J, Schroeder P. Role of mitochondria in photoaging of human skin: the defective powerhouse model. J Investig Dermatol Symp Proc 2009;14:44–9.
[41] Greco M, Villani G, Mazzucchelli F, Bresolin N, Papa S, Attardi G. Marked aging-related decline in efficiency of oxidative phosphorylation in human skin fibroblasts. FASEB J 2003;17:1706–8.
[42] Birch-Machin MA, Tindall M, Turner R, Haldane F, Rees JL. Mitochondrial DNA deletions in human skin reflect photo- rather than chronologic aging. J Invest Dermatol 1998;110:149–52.
[43] Puntel RL, Roos DH, Grotto D, Garcia SC, Nogueira CW, Rocha JB. Antioxidant properties of Krebs cycle intermediates against malonate pro-oxidant activity in vitro: a comparative study using the colorimetric method and HPLC analysis to determine malondialdehyde in rat brain homogenates. Life Sci 2007;81:51–62.
[44] Danson MJ. Dihydrolipoamide dehydrogenase: a 'new' function for an old enzyme? Biochem Soc Trans 1988;16:87–9.
[45] Adam-Vizi V, Tretter L. The role of mitochondrial dehydrogenases in the generation of oxidative stress. Neurochem Int 2013;62:757–63.
[46] Shaag A, Saada A, Berger I, Mandel H, Joseph A, Feigenbaum A, et al. Molecular basis of lipoamide dehydrogenase deficiency in Ashkenazi Jews. Am J Med Genet 1999;82:177–82.
[47] Feigenbaum AS, Robinson BH. The structure of the human dihydrolipoamide dehydrogenase gene (DLD) and its upstream elements. Genomics 1993;17:376–81.
[48] Reed LJ, Oliver RM. The multienzyme alpha-keto acid dehydrogenase complexes. Brookhaven Symp Biol 1968;21:397–412.
[49] Tretter L, Adam-Vizi V. Alpha-ketoglutarate dehydrogenase: a target and generator of oxidative stress. Philos Trans R Soc Lond B Biol Sci 2005;360:2335–45.
[50] Marchi S, Giorgi C, Suski JM, Agnoletto C, Bononi A, Bonora M, et al. Mitochondria-ROS crosstalk in the control of cell death and aging. J Signal Transduct 2012;2012:329635.
[51] Starkov AA, Fiskum G, Chinopoulos C, Lorenzo BJ, Browne SE, Patel MS, et al. Mitochondrial alpha-ketoglutarate dehydrogenase complex generates reactive oxygen species. J Neurosci 2004;24:7779–88.
[52] Tretter L, Adam-Vizi V. Generation of reactive oxygen species in the reaction catalyzed by alpha-ketoglutarate dehydrogenase. J Neurosci 2004;24:7771–8.
[53] Patel MS, Hong YS. Lipoic acid as an antioxidant. The role of dihydrolipoamide dehydrogenase. Methods Mol Biol 1998;108:337–46.
[54] Carothers DJ, Pons G, Patel MS. Dihydrolipoamide dehydrogenase: functional similarities and divergent evolution of the pyridine nucleotide–disulfide oxidoreductases. Arch Biochem Biophys 1989;268:409–25.
[55] Kim YS, Podder B, Song HY. Cytoprotective effect of alpha-lipoic acid on paraquat-exposed human bronchial epithelial cells via activation of nuclear factor erythroid related factor-2 pathway. Biol Pharm Bull 2013;36:802–11.
[56] Lin YC, Lai YS, Chou TC. The protective effect of alpha-lipoic acid in lipopolysaccharide-induced acute lung injury is mediated by heme oxygenase-1. Evid Based Complement Alternat Med 2013;2013:590363.

[57] Ogborne RM, Rushworth SA, O'Connell MA. Alpha-lipoic acid-induced heme oxygenase-1 expression is mediated by nuclear factor erythroid 2-related factor 2 and p38 mitogen-activated protein kinase in human monocytic cells. Arterioscler Thromb Vasc Biol 2005;25:2100–5.
[58] Suh JH, Shenvi SV, Dixon BM, Liu H, Jaiswal AK, Liu RM, et al. Decline in transcriptional activity of Nrf2 causes age-related loss of glutathione synthesis, which is reversible with lipoic acid. Proc Natl Acad Sci U S A 2004;101:3381–6.
[59] Thakurta IG, Chattopadhyay M, Ghosh A, Chakrabarti S. Dietary supplementation with N-acetyl cysteine, alpha-tocopherol and alpha-lipoic acid reduces the extent of oxidative stress and proinflammatory state in aged rat brain. Biogerontology 2012;13:479–88.
[60] Suh JH, Wang H, Liu RM, Liu J, Hagen TM. (R)-alpha-lipoic acid reverses the age-related loss in GSH redox status in post-mitotic tissues: evidence for increased cysteine requirement for GSH synthesis. Arch Biochem Biophys 2004; 423:126–35.
[61] Wolfe RR, Jahoor F, Herndon DN, Miyoshi H. Isotopic evaluation of the metabolism of pyruvate and related substrates in normal adult volunteers and severely burned children: effect of dichloroacetate and glucose infusion. Surgery 1991;110:54–67.
[62] Robinson BH, Taylor J, Kahler SG, Kirkman HN. Lactic acidemia, neurologic deterioration and carbohydrate dependence in a girl with dihydrolipoyl dehydrogenase deficiency. Eur J Pediatr 1981;136:35–9.
[63] Robinson BH, Taylor J, Sherwood WG. Deficiency of dihydrolipoyl dehydrogenase (a component of the pyruvate and alpha-ketoglutarate dehydrogenase complexes): a cause of congenital chronic lactic acidosis in infancy. Pediatr Res 1977;11:1198–202.
[64] Brassier A, Ottolenghi C, Boutron A, Bertrand AM, Valmary-Degano S, Cervoni JP, et al. Dihydrolipoamide dehydrogenase deficiency: a still overlooked cause of recurrent acute liver failure and Reye-like syndrome. Mol Genet Metab 2013;109: 28–32.
[65] Quinonez SC, Leber SM, Martin DM, Thoene JG, Bedoyan JK. Leigh syndrome in a girl with a novel DLD mutation causing E3 deficiency. Pediatr Neurol 2013;48:67–72.
[66] McLoone P, Simics E, Barton A, Norval M, Gibbs NK. An action spectrum for the production of cis-urocanic acid in human skin in vivo. J Invest Dermatol 2005;124:1071–4.
[67] Lu YP, Lou YR, Yen P, Mitchell D, Huang MT, Conney AH. Time course for early adaptive responses to ultraviolet B light in the epidermis of SKH-1 mice. Cancer Res 1999;59:4591–602.
[68] Burstein MT, Titorenko VI. A mitochondrially targeted compound delays aging in yeast through a mechanism linking mitochondrial membrane lipid metabolism to mitochondrial redox biology. Redox Biol 2014;2:305–7.
[69] Shukla G, Bhatia M, Vivekanandhan S, Gupta N, Tripathi M, Srivastava A, et al. Serum prolactin levels for differentiation of nonepileptic versus true seizures: limited utility. Epilepsy Behav 2004;5:517–21.
[70] Krishnan KJ, Harbottle A, Birch-Machin MA. The use of a 3895 bp mitochondrial DNA deletion as a marker for sunlight exposure in human skin. J Invest Dermatol 2004;123:1020–4.
[71] Choi S, Lee SK, Kim JE, Chung MH, Park YI. Aloesin inhibits hyperpigmentation induced by UV radiation. Clin Exp Dermatol 2002;27:513–5.
[72] Yagi A, Takeo S. Anti-inflammatory constituents, aloesin and aloemannan in aloe species and effects of tanshinon VI in *Salvia miltiorrhiza* on heart. Yakugaku Zasshi 2003;123: 517–32.
[73] Yagi A, Kabash A, Okamura N, Haraguchi H, Moustafa SM, Khalifa TI. Antioxidant, free radical scavenging and anti-inflammatory effects of aloesin derivatives in *Aloe vera*. Planta Med 2002;68:957–60.
[74] Yang ZQ, Wang ZH, Zhang TL, Tu JB, Song Y, Hu XY, et al. The effect of aloesin on melanocytes in the pigmented skin equivalent model. Zhonghua Zheng Xing Wai Ke Za Zhi 2008; 24:50–3.
[75] Wang Z, Li X, Yang Z, He X, Tu J, Zhang T. Effects of aloesin on melanogenesis in pigmented skin equivalents. Int J Cosmet Sci 2008;30:121–30.
[76] Giacomoni PU. Sun protection in man. Elsevier; 2001 324–34.
[77] Park HM, Shin J, Kim JK, Lee SJ, Hwang G, Liu K, et al. MS-based metabolite profiling reveals time-dependent skin biomarkers in UVB-irradiated mice. Metabolomics 2014;10: 663–76.

Name: Eunjung Moon
Organization: Research Institute of Pharmaceutical Science, Gachon University, Incheon, Republic of Korea
Current position: Researcher
Phone: 82-10-3731-6410
Email: jubbi@hanmail.net
Education: Ph.D. in Medical Science, Graduate School of East–West Medical Science, Kyung Hee University, Republic of Korea (2013)

Name: Hye Min Park
Organization: Department of Bioscience and Biotechnology, Konkuk University, Seoul, Republic of Korea
Current position: Researcher
Phone: 82-2-444-4290
Email: ramgee@naver.com
Education: Ph.D. in Medical Science, Graduate School of East–West Medical Science, Kyung Hee University, Republic of Korea (2011)

Name: Choong Hwan Lee
Organization: Department of Bioscience and Biotechnology, Konkuk University, Seoul, Republic of Korea
Current position: Professor
Phone: 82-2-2049-6177
Email: chlee123@konkuk.ac.kr
Education: Ph.D. in Functional Metabolomics, Seoul National University, Republic of Korea (2002)
Post-Doc. In Natural Products Metabolomics, UC San Diego, USA (1996–1997)

Name: Seong-Gil Do
Organization: Life Science Research Institute, Univera, Inc., Seoul, Republic of Korea
Current position: Director, R&D center
Email: sgildo@univera.con
Education: Ph.D. in Veterinary Medicine, College of Veterinary Medicine, Seoul National University, Republic of Korea (2002)

Name: Jong-Moon Park
Organization: College of Pharmacy, Gachon University, Republic of Korea
Current position: Ph.D. Candidate
Email: bio4647@naver.com
Education: M.S. in Analytical Chemistry, Department of Chemistry, Korea University, Republic of Korea (2010)

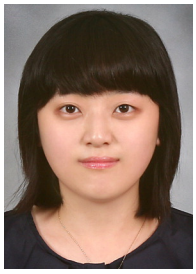

Name: Na-Young Han
Organization: College of Pharmacy, Gachon University, Republic of Korea
Current position: Ph.D. Candidate
Email: ddasehan@nate.com
Education: M.S. in Systems Medicine, Department of Proteomics, Gachon University, Republic of Korea (2011)

Name: Moon Ho Do
Organization: College of Pharmacy, Gachon University, Republic of Korea
Current position: Ph.D. Candidate
Email: dvmoono@naver.com
Education: M.S. in Oriental Medicinal Materials and Processing College of Life Science, Kyung Hee University, Republic of Korea (2012)

Name: Jong-Ha Lee
Organization: College of Pharmacy, Gachon University, Republic of Korea
Current position: Internship
Email: whdgkfl@naver.com
Education: B.S. in Pharmacy, Gachon University, Republic of Korea (2015)

Name: Hookeun Lee
Organization: College of Pharmacy, Gachon University, Republic of Korea
Current position: Professor
Email: hklee@gachon.ac.kr
Education: Ph.D. in Physical–Analytical Chemistry, Department in Chemistry, University of Utah, Utah, USA (1998)

Name: Sun Yeou Kim
Organization: College of Pharmacy, Gachon University, Republic of Korea
Current position: Professor
Phone: 82-10-2292-9232
Email: sunnykim@gachon.ac.kr
Education: Ph.D. in Pharmacy, College of Pharmacy, Seoul National University, Republic of Korea (1996)